CONTROL STRATEGY FOR ALONG-TRACK FORMATION FLIGHT TO ACHIEVE VIRTUAL TELESCOPE IN LOW EARTH ORBIT

Takeya Shima*1, Katsuhiko Yamada*2 and Shoji Yoshikawa*3

*1,*3 *Advanced Technology R&D Center, Mitsubishi Electric Corporation, Amagasaki, Japan*
*2 *Department of Aerospace Engineering, Nagoya University, Nagoya, Japan*
*1 *e-mail: Shima.Takeya@cb.MitsubishiElectric.co.jp*
*2 *e-mail: kyamada@nuae.nagoya-u.ac.jp*
*3 *e-mail: Yoshikawa.Shoji@ap.MitsubishiElectric.co.jp*

ABSTRACT

Future space missions such as virtual telescopes and interferometers require precision formation flying, i.e., a highly precise control of the relative positions of spacecrafts. This paper discusses a strategy to suppress the relative position variation during one orbit. It proposes a new approach to design a state feedback impulsive controller. By estimating the disturbance from the result of the previous control cycle and compensating for the estimated disturbance in a feed-forward manner, stable control can be achieved under uncertainties of natural disturbances. An along-track formation control in a low earth orbit is taken as an example, where the J_2 term and air drag are considered as representative natural disturbances. Numerical simulations are performed to validate the proposed controller.

NOMENCLATURE

μ_e :	gravity constant of the Earth
R_e :	equatorial radius of the Earth
J_2 :	second-order zonal harmonic coefficient of the Earth's gravitational potential ($J_2 = 1.0826 \times 10^{-3}$)
$\boldsymbol{r}$:	position vector of spacecraft in an inertia frame
a :	semimajor axis of orbit
e :	eccentricity of orbit
i :	inclination of orbit
ω :	argument of perigee of orbit
Ω :	right ascension of orbit
ν :	true anomaly of spacecraft
θ :	argument of latitude of spacecraft ($\theta = \omega + \nu$)
T :	spacecraft orbital period
I_m :	m-dimensional unit matrix
O_m :	m-dimensional zero matrix

Subscripts c and d denote the variables of a chief spacecraft and deputy spacecraft, respectively.

1. INTRODUCTION

Space science missions such as space telescopes and interferometers require a long baseline or a long focal length. Precision formation flying, in which mission components are distributed among multiple spacecrafts and the relative positions and attitudes of spacecrafts are measured and controlled with high precision, is a promising technique to satisfy this requirement[1], The achievement of precision formation flying poses many technical challenges[2]. A formation flying demonstration mission in a low earth orbit (LEO) has been proposed by several agencies as a precursor to an operational mission[3],[4],[5].

Many studies have been conducted for designing formation geometry or a relative orbit so that secular drifts due to natural disturbances are minimized[6],[7],[8],[9]. However, particularly in a LEO, the relative position variation due to the Earth's oblateness (J_2 term) is not negligible when centimeter-scale or subcentimeter-scale positional accuracy is required[10]. This paper discusses a strategy to suppress the relative position variation during one orbit under two representative natural disturbances in a LEO—J_2 disturbance and air drag. To suppress the relative position variation during one orbit, we require four key elements: 1) a highly accurate sensor, 2) highly accurate actuator, 3) suitable initial position and velocity setting, and 4) precise relative position control. This paper focuses on the fourth element using impulsive control under the J_2 disturbance and air drag.

For the suppression of the relative position variation during one orbit, initial conditions and a continuous control strategy using low thrust have been proposed by Yamada[11]. In this paper, a discrete control strategy using impulsive thrusters is proposed. A feedback control law using impulsive thrusters has already been proposed by Yamada et al.[12]. The method proposed in this study is an extension of the previous control law. It estimates the disturbance caused in a spacecraft by evaluating the result of the previous control cycle and compensates for the estimated disturbance in a feed-forward manner.

The rest of this paper is organized as follows. In section 2, the relative state transition in a Hill frame under the J_2 disturbance is discussed. The state transition matrix (STM) can be analytically obtained by the sum of two terms—the Clohessy-Wiltshire (CW) solution and a perturbation term resulting from the J_2 disturbance. In section 3, a feedback control law using impulsive thrusters is proposed. In the proposed control law, impulsive control force is calculated using a perturbed STM. The stability of the closed-loop system is shown by analyzing the eigenvalues of the system. In section 4, numerical examples of along-track formation flying in a LEO are presented. Section 5 concludes the paper.

2. STATE TRANSITION IN ALONG-TRACK FORMATION

A spacecraft that moves in a reference orbit is termed a chief spacecraft, and a spacecraft that makes a formation flight with respect to the chief spacecraft is termed a deputy spacecraft. Local orthogonal coordinates with the origin at the center of mass of the chief spacecraft are selected such that the x-axis is aligned in the direction from the Earth's center of mass to the chief spacecraft and the z-axis is aligned with the normal (rotation vector) of the orbital plane of the chief spacecraft. This local coordinate frame is termed the Hill frame.

We denote the position vector of the chief spacecraft in the inertial frame as $\boldsymbol{r}_c$ and its second derivative of time in the inertial coordinates as $\ddot{\boldsymbol{r}}_c$. The equations of motion of the chief spacecraft become as follows:

$$\ddot{\boldsymbol{r}}_c = -\frac{\mu_e}{r_c^3}\boldsymbol{r}_c + \boldsymbol{f}_{nd} \tag{1}$$

where $\boldsymbol{f}_{nd}$ is the natural disturbance force exerted on the chief spacecraft. As we consider the formation flight in a LEO, the main natural disturbance forces are given by the J_2 disturbance due to the Earth's oblateness and by air drag.

$$\boldsymbol{f}_{nd} = \boldsymbol{f}_J + \boldsymbol{f}_A \tag{2}$$

where the acceleration due to the J_2 disturbance is expressed in the Hill frame as follows:

$$\boldsymbol{f}_J = \frac{3\mu_e J_2 R_e^2}{2r_c^4}\begin{bmatrix} 3\sin^2 i_c \sin^2\theta_c - 1 \\ -\sin^2 i_c \sin 2\theta_c \\ -\sin 2i_c \sin\theta_c \end{bmatrix} \tag{3}$$

Acceleration due to air drag is given by

$$\boldsymbol{f}_A = -\frac{1}{2}\rho C_D \frac{A_c}{m_c}\|\dot{\boldsymbol{r}}_c\|\dot{\boldsymbol{r}}_c \tag{4}$$

The relative position and velocity of the deputy spacecraft with respect to the chief spacecraft are expressed in the Hill frame as

$$\boldsymbol{x} = \boldsymbol{r}_d - \boldsymbol{r}_c \tag{5}$$

$$\dot{\boldsymbol{x}} = \dot{\boldsymbol{r}}_d - \dot{\boldsymbol{r}}_c \tag{6}$$

The state vector $\boldsymbol{x}_a$ is composed of the relative position and velocity as follows:

$$\boldsymbol{x}_a = \begin{bmatrix} \boldsymbol{x}^T & \dot{\boldsymbol{x}}^T \end{bmatrix}^T \tag{7}$$

The time evolution of the state vector $\boldsymbol{x}_a$ is expressed using the STM as follows:

$$\boldsymbol{x}_a(t) = \Phi(t)\boldsymbol{x}_a(0) \tag{8}$$

where $\Phi(t)$ is the STM from time zero to time t.

Consider the case in which the chief orbit is near-circular. If we consider only the J_2 disturbance as the natural disturbance, the STM can be obtained by the sum of two terms—the CW solution and the perturbation term resulting from the J_2 disturbance.

$$\begin{bmatrix} \boldsymbol{x}(t) \\ \dot{\boldsymbol{x}}(t) \end{bmatrix} = \begin{bmatrix} \Phi_{rr}(t) & \Phi_{rv}(t) \\ \Phi_{vr}(t) & \Phi_{vv}(t) \end{bmatrix} \begin{bmatrix} \boldsymbol{x}(0) \\ \dot{\boldsymbol{x}}(0) \end{bmatrix} \tag{9}$$

$$\Phi_{rr} = \Phi_{rr}^{CW} + \Phi_{rr}^{J}, \quad \Phi_{rv} = \Phi_{rv}^{CW} + \Phi_{rv}^{J}$$

$$\Phi_{vr} = \Phi_{vr}^{CW} + \Phi_{vr}^{J}, \quad \Phi_{vv} = \Phi_{vv}^{CW} + \Phi_{vv}^{J}$$

$$\Phi_{rr}^{CW} = \begin{bmatrix} 4 - 3\cos(n_c t) & 0 & 0 \\ 6(\sin(n_c t) - n_c t) & 1 & 0 \\ 0 & 0 & \cos(n_c t) \end{bmatrix}$$

$$\Phi_{rv}^{CW} = \begin{bmatrix} \dfrac{\sin(n_c t)}{n_c} & \dfrac{2(1-\cos(n_c t))}{n_c} & 0 \\ -\dfrac{2(1-\cos(n_c t))}{n_c} & -\dfrac{3n_c t - 4\sin(n_c t)}{n_c} & 0 \\ 0 & 0 & \dfrac{\sin(n_c t)}{n_c} \end{bmatrix}$$

$$\Phi_{vr}^{CW} = \begin{bmatrix} 3n_c\sin(n_c t) & 0 & 0 \\ -6n_c(1-\cos(n_c t)) & 0 & 0 \\ 0 & 0 & -n_c\sin(n_c t) \end{bmatrix}$$

$$\Phi_{vv}^{CW} = \begin{bmatrix} \cos(n_c t) & 2\sin(n_c t) & 0 \\ -2\sin(n_c t) & -3 + 4\cos(n_c t) & 0 \\ 0 & 0 & \cos(n_c t) \end{bmatrix}$$

where n_c is the orbital angular rate of the chief spacecraft. The nonzero components of the perturbation matrix resulting from the J_2 disturbance can be analytically obtained as follows[11]:

$$\Phi_{rr}^{J}(1,1) = 2e_{c0}\left\{5(1-\cos\nu_c) - 3\nu_c\sin\nu_c\right\}$$

$$\Phi_{rr}^{J}(1,2) = \alpha(1-\cos\nu_c)\left\{\cos 2\omega_{c0}\sin\nu_c + \frac{1}{2}(2\cos\nu_c + 7)\sin 2\omega_{c0}\right\}\sin^2 i_{c0}$$

$$\Phi_{rr}^{J}(2,1) = -3e_{c0}(5\nu_c + 2\nu_c\cos\nu_c + \sin\nu_c\cos\nu_c - 4\sin\nu_c)$$

$$\Phi_{rr}^{J}(2,2) = \alpha\left\{\frac{3}{4}(1-\cos\nu_c)(1-3\cos^2 i_{c0}) - \frac{1}{4}(1-\cos\nu_c)(4\cos\nu_c + 17)\sin^2 i_{c0}\cos 2\omega_{c0}\right.$$

$$-\frac{1}{2}(9\nu_c + 2\sin\nu_c\cos\nu_c - 11\sin\nu_c)\sin^2 i_{c0}\sin 2\omega_{c0}\Big\} + e_{c0}(1-\cos\nu_c)$$

$$\begin{aligned}
\Phi^J_{rr}(3,3) &= e_{c0}(1-\cos\nu_c)\cos\nu_c \\
\Phi^J_{rv}(1,1) &= -e_{c0}\frac{2\sin\nu_c}{n_{c0}} \\
\Phi^J_{rv}(1,2) &= -e_{c0}\frac{3\nu_c\sin\nu_c - 2(1-\cos\nu_c)}{n_{c0}} \\
\Phi^J_{rv}(2,1) &= e_{c0}\frac{(\cos\nu_c+3)(1-\cos\nu_c)}{n_{c0}} \\
\Phi^J_{rv}(2,2) &= -e_{c0}\frac{3\nu_c(1+\cos\nu_c) + 2\sin\nu_c\cos\nu_c}{n_{c0}} \\
\Phi^J_{rv}(3,3) &= -e_{c0}\frac{(1+\cos\nu_c)\sin\nu_c}{n_{c0}} \\
\Phi^J_{vr}(1,1) &= 2e_{c0}n_{c0}\{2\sin\nu_c - 3(\nu_c - \sin\nu_c)\cos\nu_c\} \\
\Phi^J_{vr}(1,2) &= \alpha n_{c0}\left\{(2\cos\nu_c+1)(1-\cos\nu_c)\sin^2 i_{c0}\cos 2\omega_{c0} + \frac{1}{2}(4\cos\nu_c+5)\sin\nu_c\sin^2 i_{c0}\sin 2\omega_{c0}\right\} \\
\Phi^J_{vr}(2,1) &= 6e_{c0}n_{c0}(\cos\nu_c + \nu_c\sin\nu_c + \cos^2\nu_c - 2) \\
\Phi^J_{vr}(2,2) &= \alpha n_{c0}\Big\{\frac{3}{4}(3\sin^2 i_{c0} - 2)\sin\nu_c - \frac{1}{4}(13+8\cos\nu_c)\sin\nu_c\sin^2 i_{c0}\cos 2\omega_{c0} \\
&\quad +\frac{1}{2}(1-\cos\nu_c)(4\cos\nu_c - 7)\sin^2 i_{c0}\sin 2\omega_{c0}\Big\} + e_{c0}n_{c0}\sin\nu_c \\
\Phi^J_{vr}(3,3) &= -e_{c0}n_{c0}\sin\nu_c \\
\Phi^J_{vv}(1,1) &= -2e_{c0}(1-\cos\nu_c)\cos\nu_c \\
\Phi^J_{vv}(1,2) &= e_{c0}(-3\nu_c\cos\nu_c - \sin\nu_c + 4\sin\nu_c\cos\nu_c) \\
\Phi^J_{vv}(2,1) &= 2e_{c0}(1-\cos\nu_c)\sin\nu_c \\
\Phi^J_{vv}(2,2) &= e_{c0}(-1 + 3\nu_c\sin\nu_c - 3\cos\nu_c + 4\cos^2\nu_c) \\
\Phi^J_{vv}(2,3) &= 3\alpha(\cos^2\nu_c\cos\omega_{c0} - \cos\omega_{c0} - \sin\nu_c\cos\nu_c\sin\omega_{c0})\sin i_{c0}\cos i_{c0} \\
\Phi^J_{vv}(3,1) &= -6\alpha(1-\cos\nu_c)(\sin\omega_{c0}\cos\nu_c + \cos\omega_{c0}\sin\nu_c)\sin i_{c0}\cos i_{c0} \\
\Phi^J_{vv}(3,2) &= -3\alpha(3\nu_c\sin\nu_c\cos\omega_{c0} + 3\nu_c\cos\nu_c\sin\omega_{c0} - 4\sin\nu_c\cos\nu_c\sin\omega_{c0} - 4\cos\omega_{c0}\sin^2\nu_c)\sin i_{c0}\cos i_{c0} \\
\Phi^J_{vv}(3,3) &= e_{c0}(1-\cos\nu_c)
\end{aligned}$$

where the time variable is given by the true anomaly of the chief spacecraft and α is given by $\alpha = J_2(R_e/a_{c0})^2$. This solution assumes that the initial position of the chief spacecraft at time zero is $\nu_c = \nu_{c0} = 0$.

The following block matrices that compose the STM are defined.

$$\Phi(t) = \begin{bmatrix} \Phi_r(t) & \Phi_v(t) \end{bmatrix}, \quad \Phi_r(t) = \begin{bmatrix} \Phi_{rr}(t) \\ \Phi_{vr}(t) \end{bmatrix}, \quad \Phi_v(t) = \begin{bmatrix} \Phi_{rv}(t) \\ \Phi_{vv}(t) \end{bmatrix}$$

3. IMPULSIVE STATE FEEDBACK CONTROL

3.1 Control Logic

The state transition from time zero to time t is expressed as

$$\boldsymbol{x}_a(t) \quad = \quad \Phi(t)\boldsymbol{x}_a(0) + \int_0^t \Phi_v(t-\tau)\boldsymbol{f}(\tau)\, d\tau \tag{10}$$

Consider that the relative position $\boldsymbol{x}$ is moved to the desired position $\boldsymbol{x}_{des}$ by impulsive control using the control cycle T_C of the deputy spacecraft. Suppose that the estimate of the natural disturbance at time zero is given by $\hat{\boldsymbol{f}}_D^{(0)}$. If the impulsive force $\boldsymbol{f}_C^{(0)}$ is fired at time zero, the estimate of the state at the next firing time T_C is given by

$$\hat{\boldsymbol{x}}_a(T_C) \quad = \quad \Phi(T_C)\hat{\boldsymbol{x}}_a(0) + \Phi_v(T_C)\boldsymbol{f}_C^{(0)} + \left(\int_0^{T_C} \Phi_v(T_C - \tau)\, d\tau\right)\hat{\boldsymbol{f}}_D^{(0)} \tag{11}$$

As the impulsive force $\boldsymbol{f}_C^{(0)}$ is calculated such that the relative position $\hat{\boldsymbol{x}}(T_C)$ moves to the desired position $\boldsymbol{x}_{des}$, the following relation holds.

$$\boldsymbol{x}_{des} = \begin{bmatrix} \Phi_{rr}(T_C) & \Phi_{rv}(T_C) \end{bmatrix} \hat{\boldsymbol{x}}_a(0) + \Phi_{rv}(T_C)\boldsymbol{f}_C^{(0)} + \bar{\Phi}_{rv}(T_C)\hat{\boldsymbol{f}}_D^{(0)} \tag{12}$$

where

$$\bar{\Phi}_{rv}(T_C) = \int_0^{T_C} \Phi_{rv}(T_C - \tau)\, d\tau$$

Therefore, the impulsive force $\boldsymbol{f}_C^{(0)}$ can be obtained as follows.

$$\boldsymbol{f}_C^{(0)} = -\begin{bmatrix} \Phi_{rv}^{-1}(T_C) & I_3 \end{bmatrix} \begin{bmatrix} \Phi_{rr}(T_C)\hat{\boldsymbol{x}}(0) - \boldsymbol{x}_{des} \\ \dot{\hat{\boldsymbol{x}}}(0) \end{bmatrix} - \Phi_{rv}^{-1}(T_C)\bar{\Phi}_{rv}(T_C)\hat{\boldsymbol{f}}_D^{(0)} \tag{13}$$

The first term on the right-hand side of Eq. (13) is the feedback term and the second term is the feed-forward term for disturbance compensation. From the block structure of the feedback gain matrix in the control law (13), the gain matrix corresponding to the velocity errors becomes a unit matrix, which implies that the velocity errors are directly compensated for by the impulsive forces.

The result of the impulsive control at time zero can be evaluated at the next control time T_C. The control error that expresses the relative position deviation from the desired value can be defined as follows:

$$\delta\boldsymbol{x}(T_C) = \boldsymbol{x}(T_C) - \boldsymbol{x}_{des} \tag{14}$$

where $\boldsymbol{x}(T_C)$ obeys the following dynamics.

$$\boldsymbol{x}(T_C) = \begin{bmatrix} \Phi_{rr}(T_C) & \Phi_{rv}(T_C) \end{bmatrix} \boldsymbol{x}_a(0) + \Phi_{rv}(T_C)\boldsymbol{f}_C^{(0)} + \int_0^{T_C} \Phi_{rv}(T_C - \tau)\boldsymbol{f}(\tau)\, d\tau \tag{15}$$

Then, by subtracting Eq. (12) from Eq. (15), the control error at the next control time T_C can be evaluated as follows:

$$\delta\boldsymbol{x}(T_C) = \begin{bmatrix} \Phi_{rr}(T_C) & \Phi_{rv}(T_C) \end{bmatrix} (\boldsymbol{x}_a(0) - \hat{\boldsymbol{x}}_a(0)) + \int_0^{T_C} \Phi_{rv}(T_C - \tau)(\boldsymbol{f}(\tau) - \hat{\boldsymbol{f}}_D^{(0)})\, d\tau \tag{16}$$

where the first term on the right-hand side represents the effect of the measurement error of the state and the second term represents the effect of the estimation error of the disturbance. From the relation in Eq. (16), the estimate of the disturbance at the next control time T_C is updated as follows:

$$\hat{\boldsymbol{f}}_D^{(T_C)} = \hat{\boldsymbol{f}}_D^{(0)} + \beta\bar{\Phi}_{rv}^{-1}(T_C)\delta\boldsymbol{x}(T_C) \tag{17}$$

where β is the scalar gain for the estimation of the disturbance, and it satisfies $0 < \beta < 2$.

We decompose the natural disturbance $\boldsymbol{f}(t)$ into two terms—a constant term $\boldsymbol{f}_{const}$ that does not depend on time and a residual term $\boldsymbol{f}_{res}$ that depends on time.

$$\boldsymbol{f}(t) = \boldsymbol{f}_{const} + \boldsymbol{f}_{res}(t) \tag{18}$$

Then, the estimation error of the disturbance $\boldsymbol{f}_{const}$ obeys the following dynamics after Eq. (17) is updated.

$$\begin{aligned} \hat{\boldsymbol{f}}_D^{(T_C)} - \boldsymbol{f}_{const} \quad &= \quad (1-\beta)(\hat{\boldsymbol{f}}_D^{(0)} - \boldsymbol{f}_{const}) \\ &+\beta\bar{\Phi}_{rv}^{-1}(T_C)\left(\int_0^{T_C} \Phi_{rv}(T_C - \tau)\boldsymbol{f}_{res}(\tau)\, d\tau + \begin{bmatrix} \Phi_{rr}(T_C) & \Phi_{rv}(T_C) \end{bmatrix} (\boldsymbol{x}_a(0) - \hat{\boldsymbol{x}}_a(0))\right) \end{aligned} \tag{19}$$

This relation shows that the estimation error of the disturbance $\boldsymbol{f}_{const}$ decreases if the gain β satisfies the condition that $0 < \beta < 2$.

3.2 Stability of Closed-loop System

Consider that the stability of the closed-loop system under the control law expressed by Eqs. (13) and (17). An error vector is composed of the deviation from the desired relative position, the relative velocity, and the estimation error of the disturbance, as follows:

$$\boldsymbol{z}(t) = \begin{bmatrix} \delta\boldsymbol{x}(t) \\ \dot{\boldsymbol{x}}(t) \\ \hat{\boldsymbol{f}}_D^{(t)} - \boldsymbol{f}_{const} \end{bmatrix} = \begin{bmatrix} \boldsymbol{x}(t) - \boldsymbol{x}_{des} \\ \dot{\boldsymbol{x}}(t) \\ \hat{\boldsymbol{f}}_D^{(t)} - \boldsymbol{f}_{const} \end{bmatrix} \tag{20}$$

Then, the control error at time T_C can be evaluated as follows:

$$\begin{aligned} \delta\boldsymbol{x}(T_C) &= \bar{\Phi}_{rv}(T_C)(\boldsymbol{f}_{const} - \hat{\boldsymbol{f}}_D^{(0)}) + \int_0^{T_C} \Phi_{rv}(T_C - \tau)\boldsymbol{f}_{res}(\tau)\ d\tau \\ &\quad + \begin{bmatrix} \Phi_{rr}(T_C) & \Phi_{rv}(T_C) \end{bmatrix} (\boldsymbol{x}_a(0) - \hat{\boldsymbol{x}}_a(0)) \end{aligned} \tag{21}$$

$$\begin{aligned} \dot{\boldsymbol{x}}(T_C) &= \Phi_{vr}(T_C)\boldsymbol{x}(0) + \Phi_{vv}(T_C)\Phi_{rv}^{-1}(T_C)\left[\boldsymbol{x}_{des} - \Phi_{rr}(T_C)\boldsymbol{x}(0)\right] \\ &\quad + \int_0^{T_C} \Phi_{vv}(T_C - \tau)\boldsymbol{f}(\tau)\ d\tau - \Phi_{vv}(T_C)\Phi_{rv}^{-1}(T_C)\bar{\Phi}_{rv}(T_C)\hat{\boldsymbol{f}}_D^{(0)} \\ &\quad + \Phi_{vv}(T_C)(\dot{\boldsymbol{x}}(0) - \dot{\hat{\boldsymbol{x}}}(0)) + \Phi_{vv}(T_C)\Phi_{rv}^{-1}(T_C)\Phi_{rr}(T_C)(\boldsymbol{x}(0) - \hat{\boldsymbol{x}}(0)) \end{aligned} \tag{22}$$

By substituting the relation

$$\boldsymbol{x}(0) = \boldsymbol{x}_{des} + \delta\boldsymbol{x}(0) \tag{23}$$

into the right-hand side of Eq. (22) and using the relation

$$\boldsymbol{x}_{des} - \Phi_{rr}(T_C)\boldsymbol{x}_{des} \approx O(J_2) \tag{24}$$

$$\Phi_{vr}(T_C)\boldsymbol{x}_{des} \approx O(J_2) \tag{25}$$

of along-track formation ($\boldsymbol{x}_{des} = \begin{bmatrix} 0 & * & 0 \end{bmatrix}^T$), the following error equation can be derived.

$$\begin{aligned} \boldsymbol{z}(T_C) &= A\boldsymbol{z}(0) + \boldsymbol{b} \\ A &= \left[\begin{array}{c|c|c} O_3 & O_3 & -\bar{\Phi}_{rv}(T_C) \\ \hline \Phi_{vr}(T_C) - \Phi_{vv}(T_C)\Phi_{rv}^{-1}(T_C)\Phi_{rr}(T_C) & O_3 & -\Phi_{vv}(T_C)\Phi_{rv}^{-1}(T_C)\bar{\Phi}_{rv}(T_C) \\ \hline O_3 & O_3 & (1-\beta)I_3 \end{array}\right] \\ \boldsymbol{b} &= \begin{bmatrix} \boldsymbol{b}_p^T & \boldsymbol{b}_v^T & \boldsymbol{b}_f^T \end{bmatrix}^T \\ \boldsymbol{b}_p &= \bar{\Phi}_{rv}(T_C)(\boldsymbol{f}_{const} - \hat{\boldsymbol{f}}_D^{(0)}) + \int_0^{T_C} \Phi_{rv}(T_C - \tau)\boldsymbol{f}_{res}(\tau)\ d\tau \\ &\quad + \begin{bmatrix} \Phi_{rr}(T_C) & \Phi_{rv}(T_C) \end{bmatrix} (\boldsymbol{x}_a(0) - \hat{\boldsymbol{x}}_a(0)) \\ \boldsymbol{b}_v &= \bar{\Phi}_{rv}(T_C)\boldsymbol{f}_{const} - \Phi_{vv}(T_C)\Phi_{rv}^{-1}(T_C)\bar{\Phi}_{rv}(T_C)\hat{\boldsymbol{f}}_D^{(0)} \\ &\quad + \int_0^{T_C} \Phi_{vv}(T_C - \tau)\boldsymbol{f}_{res}(\tau)\ d\tau \\ &\quad + \Phi_{vv}(T_C)\Phi_{rv}^{-1}(T_C)\Phi_{rr}(T_C)(\boldsymbol{x}(0) - \hat{\boldsymbol{x}}(0)) + \Phi_{vv}(T_C)(\dot{\boldsymbol{x}}(0) - \dot{\hat{\boldsymbol{x}}}(0)) + O(J_2) \\ \boldsymbol{b}_f &= \beta\bar{\Phi}_{rv}^{-1}(T_C) \\ &\quad \left(\int_0^{T_C} \Phi_{rv}(T_C - \tau)\boldsymbol{f}_{res}(\tau)\ d\tau + \begin{bmatrix} \Phi_{rr}(T_C) & \Phi_{rv}(T_C) \end{bmatrix} (\boldsymbol{x}_a(0) - \hat{\boldsymbol{x}}_a(0))\right) \end{aligned} \tag{26}$$

where the vector $\boldsymbol{b}$ is composed of the residual vector of feed-forward compensation, the measurement error of the relative position, and the relative velocity. Therefore, the stability of the closed-loop system can be determined by calculating the eigenvalues of the matrix A. If all the eigenvalues of the matrix A exist in a unit circle, the closed-loop system becomes stable. From the block structure of matrix A, it is found that the matrix has six zero eigenvalues and three $(1-\beta)$ eigenvalues. Therefore, the closed-loop system becomes stable by the impulsive control using the constant control cycle T_C.

3.3 Effect of Thruster Error

The stability analysis in subsection 3.2 corresponds to the nominal case that the thruster error is not considered. However, as large uncertainty exists in the thruster force, the range of the gain β in Eq. (17) is limited. The effect of matrix A in the presence of the thruster error can be analyzed as follows.

Suppose that the thruster force is given by

$$\boldsymbol{f}_C^{(0)*} = (1+\gamma)\boldsymbol{f}_C^{(0)} \tag{27}$$

where γ represents the thruster error. In this situation, matrix A in the error equation is given by the following matrix A^*.

$$A^* = A + \Delta A \tag{28}$$

$$\Delta A = -\gamma \left[\begin{array}{c|c|c} \Phi_{rr}(T_C) & \Phi_{rv}(T_C) & \bar{\Phi}_{rv}(T_C) \\ \hline \Phi_{vv}(T_C)\Phi_{rv}^{-1}(T_C)\Phi_{rr}(T_C) & \Phi_{vv}(T_C) & \Phi_{vv}(T_C)\Phi_{rv}^{-1}(T_C)\bar{\Phi}_{rv}(T_C) \\ \hline \beta\bar{\Phi}_{rv}^{-1}(T_C)\Phi_{rr}(T_C) & \beta\bar{\Phi}_{rv}^{-1}(T_C)\Phi_{rv}(T_C) & \beta I_3 \end{array}\right]$$

Therefore, all the eigenvalues of matrix A^* that exist in a unit circle are required for the gain β, which depends on the uncertainty γ.

4. NUMERICAL EXAMPLES

Along-track formation control in a LEO is taken as an example. The parameters of the chief and deputy spacecrafts in the numerical simulation are shown in Table 1.

Table 1 Mass properties of spacecrafts

Item	Chief	Deputy	Unit
Mass	400	350	[kg]
Cross section	5.0	5.0	[m^2]

Initial orbital elements of the chief spacecraft at time zero are given by

$$a_{c0} = 6878 \text{ [km]},\ e_{c0} = 0,\ i_{c0} = 45 \text{ [deg]},\ \Omega_{c0} = 0 \text{ [deg]},\ \omega_{c0} = 0 \text{ [deg]},\ \theta_{c0} = 0 \text{ [deg]}$$

In the initial state, the deputy spacecraft is at rest at a position 30 m ahead of the chief spacecraft. The relative position and velocity of the deputy spacecraft are expressed in the Hill frame as follows:

$$\boldsymbol{x}(0) = \begin{bmatrix} 0 & 30 & 0 \end{bmatrix}^T \text{ [m]},\quad \dot{\boldsymbol{x}}(0) = \begin{bmatrix} 0 & 0 & 0 \end{bmatrix}^T \text{ [m/s]}$$

The air density and coefficient of air drag are given by

$$\rho = 5 \times 10^{-13} \text{ [kg/m}^3\text{]},\quad C_D = 2.0$$

Figure 1 shows the relative position variation (x and y components in the Hill frame) under free orbital motion during one orbit. Figure 1 (left) shows the case in which only the J_2 disturbance is considered as the natural disturbance. Figure 1 (right) shows the case in which both the J_2 disturbance and air drag are considered as natural disturbances. From this figure, the following observations are made:

- Periodic variation due to the J_2 disturbance, whose peak-to-peak amplitudes are approximately 2 cm (x-direction) and 11 cm (y-direction), is observed from the curves on the left-hand side of Figure 1.
- A secular drift in both the x-direction and y-direction due to air drag is observed from the curves on the right-hand side of Figure 1.

In the case of a telescope mission, for example, where centimeter-scale or subcentimeter-scale accuracy is required in formation flying, the relative position variation during one orbit is not negligible and it is necessary to suppress the variation by a control strategy.

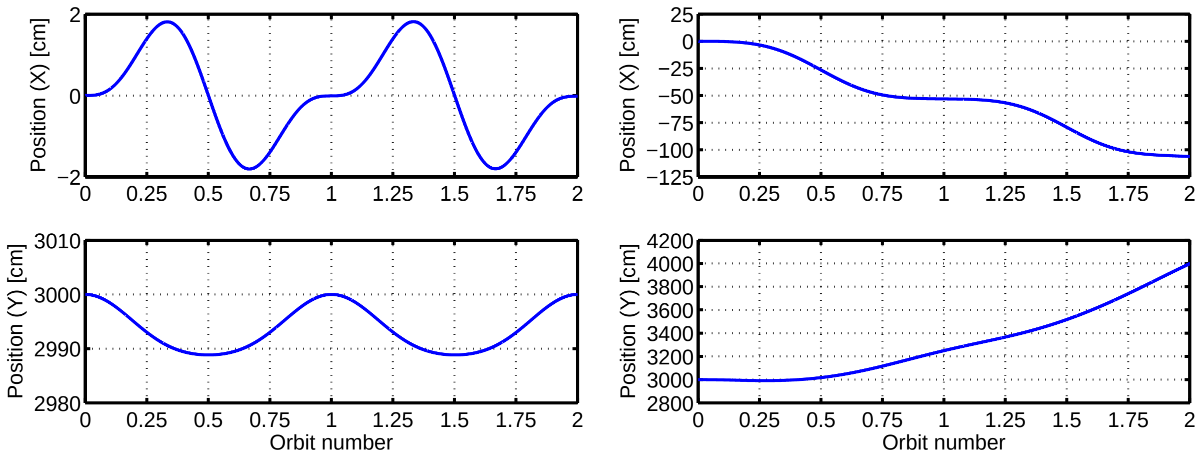

Fig. 1 Relative position variation in free orbital motion during one orbit
(Left: J_2 disturbance is considered: right: Both J_2 and air drag are considered)

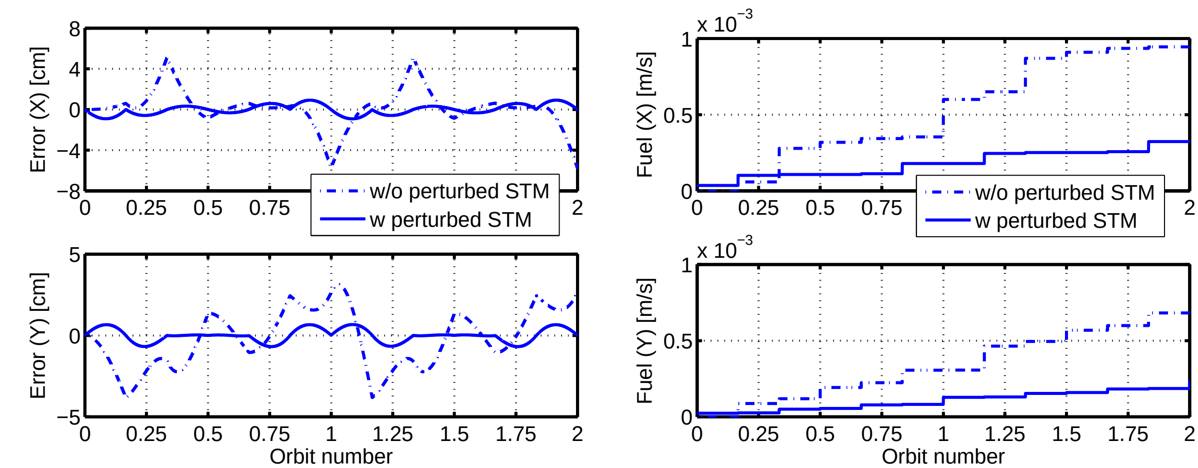

Fig. 2 Comparison between results obtained with and without perturbed STM
(Left: Relative position error: right: Fuel consumption)
(Control cycle is $T_C = T/6$ and gain is $\beta = 0$)
(Only the J_2 disturbance is considered)

Figure 2 shows the simulation result obtained by the proposed control law when only the J_2 disturbance is considered. The left-hand side of the figure shows the relative position error and the right-hand side of the figure shows the fuel consumption. The chain line shows the result of the impulsive control where the nominal STM based on the CW solution is used. The solid line shows the result where the perturbed STM resulting from the J_2 disturbance is used. The control cycle T_C is $T_C = T/6$ where T is an orbital period. The following observations are made:

- When the nominal STM is used, the relative position variation is approximately 5 cm. On the other hand, when the perturbed STM is used, the relative position variation is suppressed to within approximately 1 cm. Furthermore, the periodic nature of the relative motion is conserved after the control is achieved. This is natural because the J_2 disturbance is periodic. It is considered that natural control is achieved by the proposed controller. This is also confirmed from the result that the fuel consumption is suppressed more in the perturbed controller than it is in the nominal controller.

Now, we consider the selection of the gain β in the case that both the J_2 disturbance and air drag are considered. Figure 3 shows the stability range of the gain β versus the thruster error γ. The dashed line shows the case for $T_C = T/4$. The solid line shows the case for $T_C = T/6$. The chain line shows the case for $T_C = T/8$. It is observed that the stability range of the gain β depends on the thruster error and control cycle.

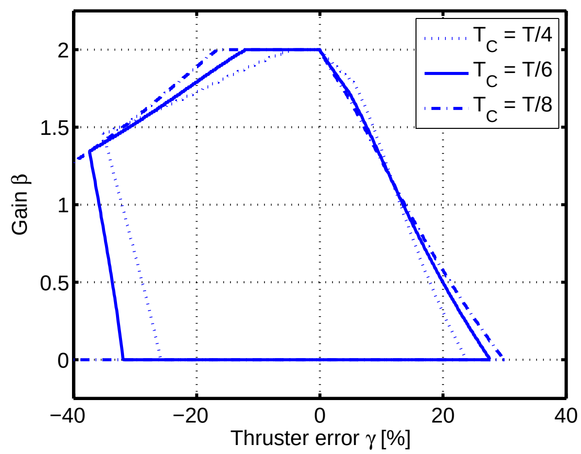

Fig. 3 Stability range of gain β vs. thruster error γ

We assume that the control cycle is $T_C = T/6$ and the gain is $\beta = 0.5$. Figure 4 shows the result in the nominal case in which the thruster error is given by $\gamma = 0$. The chain line shows the result for $\beta = 0$ where the disturbance is not compensated for. The solid line shows the result for $\beta = 0.5$ where the disturbance is compensated for in a feed-forward manner. The perturbed STM is used in both controllers. From this figure, the following observations are made:

- If the gain β is given by $\beta = 0$, the residual bias error due to air drag exists in both the x-direction and the y-direction in the Hill frame. On the other hand, if the gain β is given by $\beta = 0.5$, no residual bias error is present.

- If the feed-forward compensation is used, the fuel consumption in the x-direction is suppressed to a large extent. If the feed-forward compensation is not used, the error in both the x-direction and the y-direction is compensated for by the feedback control, as a result of which more fuel is consumed.

Figure 5 shows the result for $\gamma = -0.2$. The trend of the relative motion is the same as that of the relative motion shown in Figure 4: a stable behavior of the control is obtained by selecting a suitable gain β.

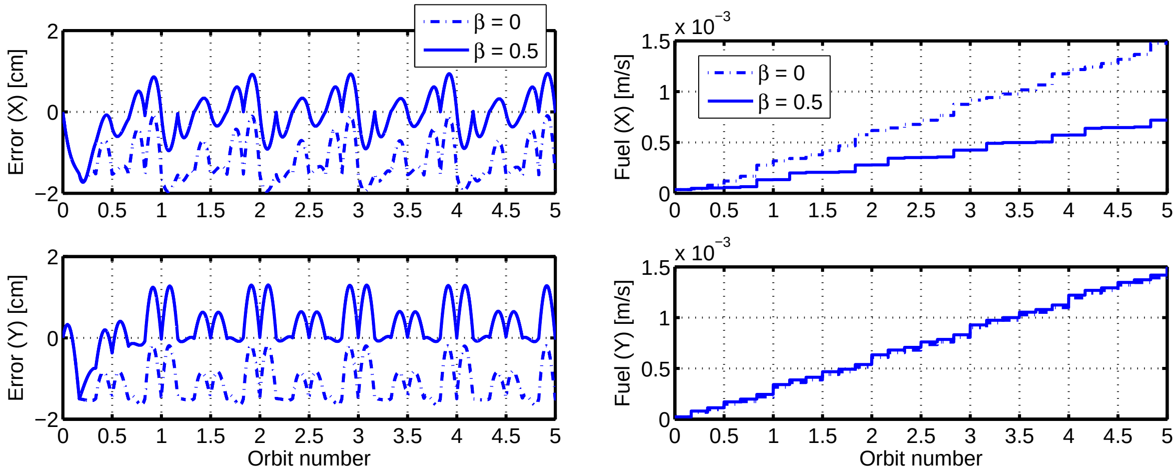

Fig. 4 Comparison between cases with and without feed-forward compensation ($\gamma = 0$)
(Left: Relative position error: right: Fuel consumption)
(J_2 and air drag are considered. Control cycle is $T_C = T/6$)

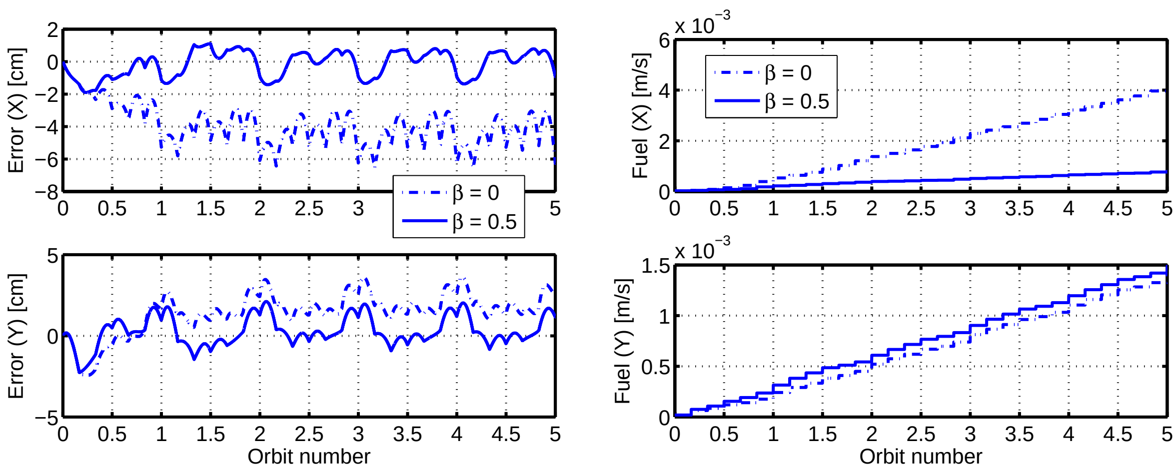

Fig. 5 Comparison between cases with and without feed-forward compensation ($\gamma = -0.2$)
(Left: Relative position error: right: Fuel consumption)
(J_2 and air drag are considered. Control cycle is $T_C = T/6$)

5. CONCLUSION

In this paper, we have discussed a strategy for suppressing the relative position variation during one orbit in along-track formation flying in a LEO. We have proposed the feedback control strategy using impulsive thrusters. By using a perturbed STM in which the effect of the J_2 disturbance is considered, periodic impulsive control in which the fuel consumption is suppressed is achieved. By estimating the disturbance from the result of the previous control cycle and compensating for the estimated disturbance in a feed-forward manner, stable control with no bias error can be achieved under the uncertainties of natural disturbances such as air drag. The effectiveness of the proposed control strategy has been verified by numerical examples of along-track formation control.

REFERENCES

[1] Hong, J., and Hadaegh, F.Y., "Precision Formation Flying (PFF)," *Earth Science Technology Conference*, June 27, 2006.

[2] Scharf, D.P., "Precision Formation Flying Missions and Technologies," *9th Briefing for Industry*, JPL, 2008.

[3] "In Orbit Formation Flying Experiment for PROBA 2: Feasibility Study," Surrey Satellite Technology Ltd.

[4] Leitner, J., et al., "A Concept for In-space, System-level Validation of Spacecraft Precision Formation Flying," *Proceedings of AIAA Guidance, Navigation and Control Conference and Exhibit*, Hilton Head, 2007.

[5] Tsunemi, H., et al., "Formation Flight All Sky Telescope (FFAST)," *Proceedings of SPIE*, Vol. 5900, 2005, pp. 184–194.

[6] Nakasuka, S., et al., "Study on the Relative Motion and Orbit Design for Clustered Satellite," *4th Workshop on Astrodynamics and Flight Mechanics*, 1994, pp. 88–92.

[7] Inalhan, G., et al., "Relative Dynamics and Control of Spacecraft Formations in Eccentric Orbits," *Journal of Guidance, Control and Dynamics*, Vol. 25, No. 1, 2002, pp. 48–59.

[8] Gim, D.W., et al., "State Transition Matrix of Relative Motion for the Perturbed Noncircular Reference Orbit," *Journal of Guidance, Control and Dynamics*, Vol. 26, No. 6, 2003, pp. 956–971.

[9] Sabatini, M., et al., "Special Inclinations Allowing Minimal Drift Orbits for Formation Flying Satellites," *Journal of Guidance, Control and Dynamics*, Vol. 31, No. 1, 2008, pp. 94–100.

[10] Yoshikawa, S., Shima, T., and Yamada, K., "Suppression of Relative Position Variation during One Orbit for Precise Formation Flying," *Proceedings of the 26th International Symposium on Space Technology and Science*, Hamamatsu, Japan, 2008.

[11] Yamada, K., "Analysis of Formation Flying with Low Thrust," *JAXA-SP-07-020*, 2008, pp. 39–48 (in Japanese).

[12] Yamada, K., Yoshikawa, S., and Nishiyama, T., "On Relative Position Control between Two Spacecraft," *Transactions of the Japan Society of Mechanical Engineers*, Vol. 70, No. 697, 2004, pp. 2638–2645 (in Japanese).